University of Exeter coursework header sheet

Extension
072990

ECMM102 Group Project (Meng) (A, TRM1+2 2017/8)

1029797

640007215

Coursework: Individual contribution to the group achievement
Submission Deadline: Mon 14th May 2018 12:00
Personal tutor: Ms Aileen Macgregor

Marker name: Tabor
Word count: 15358

By submitting coursework you declare that you understand and consent to the University policies regarding plagiarism and mitigation (these can be seen online at www.exeter.ac.uk/plagiarism, and www.exeter.ac.uk/mitigation respectively), and that you have read your school's rules for submission of written coursework, for example rules on maximum and minimum number of words. Indicative/first marks are provisional only.

First marker's comments

Indicative mark

Second marker's comments

Second mark

Moderator's comments

Agreed mark

I2 Report

Validation of Sedimentation Tanks through Empirical Studies

Abigail Baker

2018

4th year MEng Group Project

I certify that all material in this thesis that is not my own work has been identified and that no material has been included for which a degree has previously been conferred on me.

Signed..... .....

College of Engineering, Mathematics, and Physical Sciences
University of Exeter

I2 Report

ECMM102

Title: Validation of Sedimentation Tanks through Empirical Studies
Word count: 15358
Number of pages: 40

Date of submission: Monday, 14 May 2018

Student Name: Abigail Baker
Programme: MEng Mechanical Engineering
Student number: 640007215
Candidate number: 072990

Supervisor: Dr Gavin Tabor

Abstract

This report details the validation of simulation models created of two primary sedimentation tanks using empirical studies. The two sedimentation tanks studied were: an ARMFIELD W7 model rectangular sedimentation tank and a Hydrodynamic Vortex Separator (HDVS) Swirl-Flo® (property of Hydro International®).

Primary sedimentation tanks, such as the rectangular tank, aid the settling out and removal of suspended particles present in wastewater, typically by reducing the flow velocity. On the other hand, the Swirl-Flo® utilises a vortex within the tank to aid this removal. These tanks are further investigated within this project.

The empirical studies of the tanks entailed a determination of steady-state concentration and dispersed-phase mass flow rates, through filtering samples taken from the outflows of both tanks at different time periods. Flow measurements to determine velocity profiles within the tanks were taken using a propeller-meter and an Acoustic Doppler. The data processing methods for both are detailed within the report and plots were created to display the velocities.

With the provision of simulation data, further comparison plots were created comprising of simulation and empirical data for both dispersed-phase mass flow rates and velocity profiles. These found validations of the empirical data from the two instruments used along with comparisons between the Swirl-Flo® and rectangular tank. On comparison between the empirical and simulation results, similar behavioural trends within the velocity profiles and time to convergence were observed, suggesting the simulations were useful. However, the simulations were declared invalid due to large differences to the experimental data, likely due to errors in modelling conditions.

Keywords: Sedimentation Tanks; Empirical Validation; Acoustic Doppler

Table of contents

1. Introduction and background

This report details a project focused on the experimental studies and validation of two sedimentation devices: an ARMFIELD W7 model rectangular sedimentation tank and a Hydrodynamic Vortex Separator (HDVS) Swirl-Flo® (property of Hydro International®). This forms part of a larger group project whereby simulation models were created and the experimental studies were required to validate these simulations.

Within this report, research carried out into sedimentation tanks and vortex separators, as well as research and information on various methods for determination of flow velocities and concentration are detailed in the form of a literature review. The methods for the experiments carried out, as well as those for the analysis of the data collected are outlined and the results of these clearly displayed.

1.1. Wastewater Separation

Wherever humans are found waste is produced. In particular, where there are large congregations of humans the disposal of waste grows in importance. Sewage, or wastewater, is defined as "waste matter such as water or human urine or solid waste," [1], and the removal of this is key for a good quality of living and for the health of the community. Where wastewater is untreated, or ineffectively disposed of, it can quickly become a breeding ground of various pathogens, leading to outbreaks of serious water-born diseases such as cholorea and typhoid fever. Furthermore, if wastewater gets into local waterways, the local ecosystem can be disrupted, potentially causing long-term damage to the environment and the organisms that live there.

This means that there is heightened importance for the safe treatment and disposal of sewage, or wastewater and in developed countries, such as the United Kingdom, there are in place strategies for doing so efficiently in different stages. These stages are commonly denoted as: preliminary and primary, secondary and tertiary (which in some cases can be broken further into advanced and disinfection) [2]. This project focuses on the methods and in particular two examples of tanks that are utilised in the primary stage, which is the initial separaration of solids, although all stages are explained in Section 2.1.

1.2. Group Project Overview

As mentioned previously, this project forms a part of a larger group project. The overall aim of this group project was to develop CFD models and simulations of the two aforementioned tanks which accurately model the flow of wastewater. To do this, it was

proposed that properties of a sludge substitute be determined, and the flow of this wastewater substitute be validated, the sludge substitute being olivestone powder (OSP).

This group project was broken down into 4 main objectives:

- To determine the characteristics (rheology and settling velocity) of the olivestone powder and water mixture.
- To create CAD geometries of the sedimentation devices and mesh the internal domains. Compare different meshing software and investigate mesh parameters and automation.
- To perform CFD simulations of the sedimentation devices using the CFD code OpenFOAM®.
- To validate the CFD simulations with experimental studies, carried out in a controlled laboratory environment.

To achieve these objectives, the following deliverables were identified:

- An in-depth literature review of wastewater modelling techniques.
- A mathematical model for both the rheological and settling velocity behaviour of an olivestone and water suspension.
- CAD geometries of the sedimentation devices with meshed internal domains.
- A Comparison of automated and bottom-up meshing approaches.
- A documented understanding of the parameters enabling good mesh quality generation on irregular geometries.
- Two empirically studied and compared sedimentation devices.
- Two-phase CFD simulations of both sedimentation devices.
- An experimentally validated CFD model for the behaviour of a sedimentation device, using an OSP and water suspension.
- A set of design improvements from the CFD and experimental studies.

Each group member was allocated a different aspect of the project, with an emphasis either on the experimental work or simulation work.

1.3. Experimental Studies and Validation

This report details information on the experimental studies and validation project. This project achieves the group objectives and deliverables:

- To validate the CFD simulations with experimental studies, carried out in a controlled laboratory environment.

- Two empirically studied and compared sedimentation devices.

This report also aids with the completion of the deliverable:

- An experimentally validated CFD model for the behaviour of a sedimentation device, using an OSP and water suspension.

In addition to these group objectives and deliverables, this report provides an in-depth literature review of different flow-measurement techniques as well as a comparison and evaluation of two of these techniques. This report also details the methodology for the experimental studies carried out by the experimental sub-team as well as the data analysis methods used.

2. Literature review

This project drew on a vast array of research to build up a background knowledge and understanding of key concepts. This section details a review of the research carried out as well as how it influenced and guided the project.

2.1. Wastewater Treatment

As mentioned previously in Section 1.1, wastewater treatment is commonly broken down into three key stages: primary, secondary and tertiary. A preliminary stage is commonly added: This filters out large forms of debris such as vegetation and plastic bags.

After preliminary screening, the wastewater enters the primary stage. During this stage it enters a primary sedimentation tank, where sedimentation is encouraged by slightly reducing the flow, although as shown with the Swirl-Flo, this flow rate is still close to 1L/s. In the primary sedimentation tank, solids settle to the base of the tank to form a sludge bed, while floating material may be removed from the surface.

The next processing stage is the secondary stage. At this point, aerobic biological processes are typically used to degrade and metabolise the organic matter present [2]. This stage focuses on treating the effluent, or the overflow from the primary tank and not the sludge. In this stage most solids are removed. However, as microorganisms and bacteria are often used, care must be taken to ensure these have also been removed.

The third and processing stage is the advanced or final stage. During this stage, the microorganisms utilised in the secondary stage are removed. This may be done by allowing the bacteria to settle out, creating another sludge bed that this time can be reused within the secondary stage [3]. Another common way of removing these microorganisms uses a

disinfectant, such as ultraviolet light, to cause the microorganisms to break down [2]. Furthermore, other treatments carried out in this stage focus on removing any solids that remain after the secondary process through chemical or biological processes, and sometimes even filtration of the wastewater [2].

Finally the sludge removed in the primary stage also requires further processing, however this sludge is often recycled and utilised in agricultural fertilisation of plants or even in biogas powerplants [3].

2.2. Sedimentation Tanks

As referenced in Section 2.1, sedimentation or settlement tanks are used throughout the different waste processing stages. Despite the difference between the primary and secondary processes, the basic design and structure of the tanks at both stages is similar [4]. However, as this project focuses on the validation of CFD models for two primary sedimentation tanks, further referal to sedimentation tanks will refer to, unless otherwise stated, primary tanks. These primary sedimentation tanks remove approximately 60% of suspended solids.[5]

Primary sedimentation tanks are designed to "reduce the velocity of the wastewater flow, allowing heavier organic solids (called raw sludge) to settle. (…) Scrapers present in the tank move continuously along the floor of the tank to deposit the raw sludge in hoppers for removal"[5]. Sedimentation tanks can be allocated into a variety of types. These include primary and secondary tanks, this description denoting the differences in application within the wastewater treatment process. Further types denote differences in tank shape and method of operation [6].

Tanks are commonly limited to circular, rectangular and hopper-bottom shapes. Circular tanks enable radial flow and typically the wastewater flows into the tank through a central pipe, with a vertical flow operation. Additionally, mechanical scrapers may collect the sludge which is then removed through a pipe. Rectangular tanks enable a horizontal flow along the length of the tank, and occasionally baffle walls are provided. In hopper bottom tanks, a deflector box is located next to the inlet pipe, deflecting the wastewater downwards. This results in sludge collecting at the bottom, and then being removed by a pump [6].

In terms of operation methods, tanks may either be fill and draw type or continuous flow. For fill and draw operation, a tank is filled and stored for a period of time. During that time period, the suspended particles settle to the bottom of the tank, forming the sludge bed. After the time period, the water is discharged then the settled particles are removed. Alternatively, in a continuous flow operation the water is continuously flowing at a low velocity during which the suspended particles settle to the bottom of the tank. Depending on the shape of the

tank, the flow may be either horizontal or vertical. A rectangular tank typially has continuous horizontal flow along the tank length, with a length to width ratio of at least 3:1 [7]. A circular tank typically has continuous vertical flow, with a hopper bottom provided to remove the sludge bed [6].

Both tanks studied in this project use continuous flow, with the rectangular tank having continuous horizontal flow along its length. Modifications were made to the rectangular tank at the wish of the industrial contact from Hydro International® to include a hopper and an inclined base. The Swirl-Flo® is a novel application of a vortex separator as a primary tank created by Hydro International® and as such it exhibits different behaviour to a typical circular tank, observed further through later empirical studies.

2.3. Vortex Separators and Hydrocyclones

Vortex separators utilise cyclonic technology, centrifugal forces in a vortex generated by rotational movement, to separate out particles or fluids of differing density. Hydrocyclones apply vortex separation within liquids to remove either small solid particles, such as OSP, or less dense liquids such as oil from a liquid such as water. Further applications of vortex separation occur in other technologies utilising the same techniques in other mediums such as air to remove particles from said medium, for example within Dyson vacuum cleaners [8]. Within the wastewater processing world, Hydro International® utilise vortex separation within many products involved in the treatment and processing of water [9].

Hydrocyclones function by pumping a fluid through a tangential inlet near the top, This fluid then flows in a helical flow pattern down to the base of the hydrocyclone. At the base, the denser fluid is removed through an underflow, while the rest reverses direction and takes a helical flow pattern up to the overflow [10]. The Swirl-Flo® functions in a similar way, however there are some slight differences in design to that of a traditional hydrocyclone. These cannot be further described here due to Intellectual Property (IP) constraints.

2.4. Steady-State Concentration Determination

A key element sought for identification in both the empirical and simulation studies was steady-state concentration. Within this project, steady-state concentration is defined as the point at which the concentration values (regarding the concentration of OSP in the water) at the overflows and underflows do not greatly differ over time (greatly being outside of the absolute error range). The time taken to steady-state concentration was identified as the point where the plots of concentration against time converged. Examples of these plots are shown in Section 4.2.

To determine steady-state concentration a few methods are commonly used. Many of these entail the use of different filtering methods and measuring the mass of the dried sample, however turbidity meters may also be used in addition. Turbidity meters work by emitting a known intensity of light into a sample. The particles in the sample absorb the light or scatter it and the scattered light is picked up by a photodetector which converts the signal into a concentration measurement. Recently, turbidity methods have been modified to use the measurement principle of nephelometry, whereby the scattered light is measured at an angle of 90º resulting in the development of a nephelometer turbidity meter. The units of the data from this device are NTU (Nephelometric Turbidity Unit) [11].

2.5. Flow Measurement Techniques

There are many different methods and techniques for measuring flow rates and velocities of liquids, some more commonly used than others. Over time, older methods have been modified and improved and new methods developed using a variety of new technology. This section details some of these techniques.

2.5.1. Lasers and LEDs

Over time a large array of techniques that utilise lasers have been developed, the key ones being: Particle Image Velocimetry (PIV), Laser Doppler Anemometry (LDA) (also known as Laser Doppler Velocimetry (LDV), Laser-Induced Fluorescence in Liquid Phase Flows (LIF) and Particle Tracking Velocimetry (PTV) [12].

PIV is an optical technique that is non-intrusive to the flow. Two velocity components are determined through the measurement of movement of particles between two light pulses. The flow is illuminated by a light sheet and a sensory array on a digital camera enables the capture of each light pulse [12].

LDA or LDV is another technique that is non-intrusive to the flow. This method requires 1 continuous wave laser to be split into 2 beams of equal intensity but different frequencies, which are then focused and modulated to produce parallel planes of high light intensity. This is directed at the flow and particles present within the fluid scatter light which is then slightly shifted in frequency by the Doppler effect and detected by a photo-detecter. From the Doppler shift and Doppler frequency of the scattered light, flow velocities may then be determined [12].

LIF requires a tracer to be added to the fluid being observed. A laser light sheet illuminates a thin plane in the flow and the tracer absorbs some of the energy, exciting it to a higher energy state, as the tracer returns to its orignal energy state, part of the energy is released as fluorescent light, which can be detected by a camera through a filter which enables the

camera to only record fluorescent light. This recording may then be used to determine the flow profile in that plane [12].

PTV enables the measurement of the velocity of low density seeded particles in a fluid by measuring the flow field in a laser sheet. The seeded particles can then be tracked individually enabing easy determination of their velocities [12].

Lasers have traditionally been used in these techniques as they provide an intense, monochromatic beam of light that is in phase. With this in mind however, recent developments have sought to use LEDs as a safer alternative to lasers [13].

2.5.2. Nuclear Magnetic Resonance

The Nuclear Magnetic Resonance (NMR) technique uses the same principle as Magnetic Resonance Imaging (MRI). Commonly this technique is used to measure blood flow. A velocity distribution function is obtained by using magnetic fields to examine the spin of atoms, and from various calculations the number of molecules per velocity interval can be calculated as well as the total velocity distribution [14].

2.5.3. Acoustic Doppler

The Acoustic Doppler utilises ultrasound and the Doppler shift to obtain velocity information. A short acoustic pulse is sent from the transmitter elements and when the echo reaches the receiver elements, it is processed to find the Doppler shift. The scaling is then adjusted with the measured speed of sound in the liquid and a velocity vector is recorded.

2.5.4. Thermal Flowmeters

Thermal flowmeters commonly utilise thermocouples to measure flow velocities. A thermocouple generates an E.M.F (electromotive force) from a temperature difference between the two junctions. In a flowing fluid, the temperature difference is lower where there is a higher stream velocity. This means that a thermocouple generates an E.M.F where there is a difference in flow velocities. When interpreted from the E.M.F via sensor resistance, the stream velocity can be indicated [14].

2.5.5. Tracer Methods

Tracer methods are an older way of measuring flow, but for some key health and safety reasons regarding the radiation involved they are not commonly used any more. Tracer methods used to entail injecting a radioactive tracer into the flow and detecting the velocity using probes that detected radiation. Another similar method entailed irradiating the material present on the flow and detecting the gamma radiation that was emitted [14].

2.5.6. Electromagnetic Flowmeters

Electromagnetic flowmeters utilise inductive flow measurement to measure mean velocities. Magnetic fields can be generated by electromagnets and, as long as the flow profile is symmetrical the mean velocity and flow rate can be determined [14]. Inductive flow measurement is the same principle as electromagnetic induction, whereby when the fluid enters the magnetic field a voltage signal will be induced and detected by sensors.

2.5.7. Pressure Difference Flowmeters

An example of a pressure difference flowmeter is a Venturi flowmeter. A Venturi flowmeter applies Bernoulli's equation with a manometer to calculate the pressure drop within a pipe or an orifice, where Bernoulli's equation is used to calculate the velocity from the pressure difference shown by the manometer [15]. Similarly, pitot tubes apply Bernoulli's equation to calculate flow velocities from the difference between static and dynamic pressures and from converting kinetic energy to potential energy [14]. A manometer may be used in a similar way to a pitot tube, using a pressure difference to calculate flow rates and velocities with the additional benefit of not needing calibration before use.

2.5.8. Propeller-meters

Propeller-meters and turbine meters both have similar technologies and applications: both consist of a rotor or propeller, supported by either low-friction bearings or a spindle and both revolve at a rate proportional to the speed of flow. However the key difference is that the propeller-meter faces directly into the flow while the turbine meter is normal to the flow, much like a waterwheel. Results are typically given as the frequency of rotations, however, with a calibration chart they can easily be converted onto velocities [14].

2.5.9. Flowmeter Requirements

For any new or existing flow measuring technique, the key industry standard requirements are: repeatability, range-ability (the range of accuracy of the results), reliability, accuracy and the right price (the right cost in terms of budget and quality of results) [14]. These requirements are key for consideration when selecting what measurement techniques to use within the empirical studies and looking at adapting methods for further investigation.

2.6. Validation Processes

Experimental Validation of Computational Fluid Dynamics (CFD) is key to provide confidence in the results. As the Swirl-Flo® is a novel product, no experimental validation or CFD simulations of the tank with an OSP suspension has been carried out before and the same is true for the rectangular tank. Some work, however, has been done on the validation

of CFD predictions and modelling for cyclones [16] [17]. From this work it was observed that typical percentage differences between values relating to pressure drop was between 5% and 10% [17].

3. Theoretical Background, Experimental Work and Analysis

For completion of the project deliverables, a variety of tasks needed to be completed. This section outlines these tasks, providing details on the backgrounds, techniques and methods for each. Additionally, the health and safety issues encountered are detailed as well as problems that occurred and how they affected the project and were resolved.

3.1. Flow Measurement Techniques

From the many methods of flow measurement outlined in Section 2.4, only a few could be utilised within the experiments for a variety of reasons including cost and availability. The methods used were the: Acoustic Doppler, propeller-meter, blue dye, electronic flow meters and a manometer. Originally the rectangular tank utilised manometers to determine the flow into the tank, however due to the modifications made to the tank, the new flow rate exceeded the flow rate measurable for the inflow manometer. The Acoustic Doppler and propeller-meter were selected as instruments to use within the project as they were both readily available and were also versatile and utilised different techniques to provide velocity data. With both the instruments it was easy to take repeated measurements and the Acoustic Doppler had the ability to take measurements across a vertical range. Electronic flow meters were used as they met the repeatability, reliability, accuracy and price requirements. Blue dye was used as in qualitative experiment to observe the behaviour of the flow, with recordings taken to see if there was the potential of combining this with multiple flow measurement techniques to gain quantitative results.

The laser methods outlined in Section 2.5.1 were not utilised within the project as the health and safety issues regarding the use of lasers meant usage permission was unattainable. Exploration of the use of LEDs instead of lasers was considered however it was felt that this would distract from the main project objectives. As mentioned in Section 2.5.2, NMR techniques are commonly used in specialised applications to measure blood flow and similar, and hence would have been very expensive to implement so this method was not utilised. The thermal flowmeter outlined in Section 2.5.4 was not utilised as the results produced would have been hard to distinguish from the sensor resistance. As mentioned in Section 2.5.5, the tracer methods were not utilised due to the major health and safety implications of exposure

to radiation. The electromagnetic method outlined in Section 2.5.6, was not utilised as the flows being measured could not be assumed to be symmetrical.

3.2. Steady-State Concentration Determination

As mentioned in Section 2.4, there are two key methods by which concentration may be determined: turbidity meters or filtration. A turbidity meter was viewed as the optimal tool to use to determine when steady-state concentration had been reached. As a concentration value could be obtained faster through this method than through filtration. However, a turbidity meter was not obtainable as: there was not one owned by the university to borrow, it was an expensive to buy and none were available to hire from an external source.

Making a turbidity meter using a turbidity sensor with an Arduino Uno board. While this would have been achievable, it was discounted for various reasons, the key being that: it would distract from the main focus of the project deliverables, as well as raising many potential safety issues and permissions due to the use of a handmade electronic device in water. In addition, in an uncalibrated handmade device there was a large possibility of unknown errors building up, giving incorrect values.

Due to the aforementioned reasons, it was decided to use the longer but more reliable filtration approach to obtain sample concentrations.

3.2.1. Filtration Methodology

Samples were collected from both the overflow and underflow outflows at various times starting from when the OSP appeared in the tank (following the experimental procedure outlined in Section 3.3). These samples were then labelled with the outflow and tank the sample was taken from. The time and day it was taken was also recorded in case of a filtration backlog.

Before the filtration of the samples commenced, the filter papers used were washed with clean water and dried in a drying/curing oven then kept within an airtight container to prevent any moisture from the air dampening the papers before use. This is because it was found that the filter papers would lose some mass when water passed through them and they were dried.

The filter papers were individually numbered and then weighed, with the mass of each paper recorded. A sample was then selected and emptied into a measuring cylinder for the sample volume to be recorded, before washing the sample container out to ensure all traces of OSP were removed for filtration. The sample time and volume were recorded with the filter paper and its number. After standard filtration using a funnel was completed (with a rinsing out of the measuring cylinder to ensure all filtration of OSP), the filter paper was placed on a

tray and in the oven to dry out overnight to ensure that all moisture was removed from the OSP. When dry, the filter paper (and OSP filtrate) were weighed and the combined mass recorded, for subsequent data analysis as outlined in Section 3.4.1.

3.3. Experimental Methodology

For both the rectangular tank and the Swirl-Flo®, the experimental procedures were the same. Once the water had filled the tank, the pump for the OSP suspension and the timer for the experiment times would be started as soon as the OSP appeared in the tank.

Flow rates at the inflow and outflows would then be determined. For the rectangular tank, this was through Gardena electronic flow meters at the inflow and underflow outflow, which gave the flow rate in L/min. With valves the flow rates could be maintained at 24.2L/min at the inflow and 1.3L/min at the underflow. With the subtraction of the underflow from the inflow the overflow flow rate could be obtained as 22.9L/min. For the Swirl-Flo®, a different system was required as the flow meters could not be attached to the outflows or inflow. To determine flow rates, the time taken to collect 10L of water from each outflow was recorded and the flow rate then calculated in L/s. As flow out must be equal to flow in, the flow rate at the inflow could then be calculated. These flow rates were all recorded in a table so that the information could be used in the tank simulations.

Samples for concentration values were typically taken at 15, 30 and 45 minutes and at 1, 1.5, 2, 2.5, 3 and 4 hours after the start of each experiment, with a final sample at the end. However, during some repeats samples were taken at different times (a key example being every minute for the first 10 minutes) as a greater idea of when steady-state concentration occurred was required.

As the time to steady-state concentration was initially unknown, flow measurements were not carried out until 1.5 hours had passed to avoid affecting it. At this time, the Nixon propeller-meter measurements were carried out first, followed by the Nortek Vectrino Profiler (the Acoustic Doppler) with further information detailed in the following sections.

3.3.1. Measurement Points

For both tanks, the points where the flow was going to be measured were predetermined, so that all velocity profiles obtained in CFD and from experimental data were in the same places.

For the Swirl-Flo®, the points were determined using polar coordinates, with the origin at the centre of the tank, 71mm above water level (the base of the measurement instrument jig). 3 different radii, 10 angles and 5 depths were identified for propeller-meter cross-

measurement. Due to its size, measurements with the Acoustic Doppler, could only be taken at 1 radius, 5 angles and 4 depths, where the radius was 0.24m. Table 1 details the location of points in terms of polar coordinates and depth.

Table 1 - A table detailing the measurement points in the Swirl-Flo®

Angle (degrees)	Radius (m)			Depth (m)				
18	0.21	0.24	0.27	0.37	0.29	0.235	0.175	0.085
48	0.21	0.24	0.27	0.37	0.29	0.235	0.175	0.085
73	0.21	0.24	0.27	0.37	0.29	0.235	0.175	0.085
113	0.21	0.24	0.27	0.37	0.29	0.235	0.175	0.085
133	0.21	0.24	0.27	0.37	0.29	0.235	0.175	0.085
163	0.21	0.24	0.27	0.37	0.29	0.235	0.175	0.085
203	0.21	0.24	0.27	0.37	0.29	0.235	0.175	0.085
228	0.21	0.24	0.27	0.37	0.29	0.235	0.175	0.085
313	0.21	0.24	0.27	0.37	0.29	0.235	0.175	0.085
343	0.21	0.24	0.27	0.37	0.29	0.235	0.175	0.085

For the rectangular tank, the points were determined via Cartesian coordinates, with the origin being one of the corners. As the flow could reasonably be assumed to be symmetrical, the majority of measurement points were in one half of the tank, with a few exceptions to prove the symmetry. Table 2 details the location of points in terms of x, y and z coordinates.

Table 2 - A table detailing the measurement points in the rectangular tank

Width, x (mm)	Depth, y (mm)			Length, z (mm)								
20	55	95	135	55	135	235	335	435	535	735	935	1015
100	55	95	135	55	135	235	335	435	535	735	935	1015
195	55	95	135	55	135	235	335	435	535	735	935	1015

Due to the restriction in water availability and volume disposal each day, there was only time to run the experiment once a day with full measurements with each probe, so repeats were carried out over 3 days to enable averages to be calculated.

3.3.2. Propeller-meter Measurements

To take measurements with the propeller-meter the probe was connected to the measuring instrument and using a jig, held in each of the measurement points stated and a reading in hertz (Hz) was recorded. For the rectangular tank, the time period for measurements was also set to measure the number of rotations every 10 seconds instead of 1 as the low flow rate in the tank meant that sometimes a whole rotation took longer than 1 second.

3.3.3. Acoustic Doppler Measurements

To take measurements the Acoustic Doppler was connected to a laptop and the probe placed in the water at a measurement point. Care was taken to ensure the probe was vertical. On the computer, the Vectrino Profiler program was used to record readings for 1 minute at each point, various settings had to be altered to ensure the good quality of the measurements. Of particular interest was the bottom distance (the distance from the probe to the base of the tank), the velocities and the SNR which needed to be higher than 30 to ensure reliable readings.

3.3.4. Blue Dye Experiments

The experiments with blue dye were carried out mainly in the rectangular tank as the flow in the Swirl-Flo® meant the dye diffused into the water before it could be identified.

For the experiment, blue dye was added to a burette connected to the inflow. When the tap was opened, the blue dye entered the water and the flow behaviour was observed and filmed with a camera. Two profiles were filmed, one from the side and from above, to examine the hydraulic retention time (the time between the blue dye entering the tank to the water being completely clear).

3.4. Processing and Analysis of Experimental Data

After the data was obtained from the experiments outlined above, it required processing to obtain relevant plots of concentration and velocity. This section details the methods for processing, analysing and evaluating results.

3.4.1. Sample Concentrations

From the experiments outlined in Section 3.2, a combined mass of the sample filtrate and filter paper weight was found. By subtracting the mass of the filter paper (measured before the filtration of the sample), the mass of the olivestone powder (the filtrate) was determined. The concentration for each sample was then calculated using the following equation:

$$concentration = \frac{m}{v} \quad (1)$$

Where m is the sample mass (g), v is the sample volume (L) and the concentration is the sample concentration (g/L).

All these calculations were completed in tables using Microsoft Excel. After the concentrations were calculated, scatter plots were created to plot the concentrations against time, with the expectation of a convergence of the points to a steady concentration, enabling

an identification of the time to steady-state. Plots were created for each sample run, however an average of the results at the same time was taken to help identify outliers and give more certainty to the results.

From errors within the experimental procedure outlined earlier, where the filter papers had not been washed prior to filtration, an inaccuracy was present within some of the data. This was particularly noticeable where the measured mass of the filtrate and filter paper combined was less than the original mass of the filter paper. In a bid to salvage some of this data, 4 unused filter papers were washed and dried and the mass loss recorded for each and averaged. As the mass loss was similar (to 0.001g) this was added to all initial results. This was not a perfect solution, and so results from repeated experiments have been displayed in this report.

From these repeated experiments, further calculations were made to produce plots of comparative values to those generated by the simulations. These were alpha (the volume fraction of the OSP) and mass flow rate (g/s). To calculate alpha, the concentration was first converted to mg/L, then the following equation applied:

$$\alpha = \frac{concentration}{1000 * \rho_{OSP}} \tag{2}$$

Where α is the volume fraction of the OSP, concentration is the sample concentration (g/L) and ρ_{OSP} is the density of OSP.

To calculate the mass flow rate, the following equation was used:

$$mass\ flow\ rate = concentration\ * flow\ rate \tag{3}$$

Where concentration is measured in g/L and flow rate in (L/s).

After these calculations had been carried out similar scatter plots of these values against time were plotted to identify where convergence occurred, these plots are shown in Section 4.2.

3.4.2. Propeller-meter Data

From the experiments outlined in Section 0, a value in Hertz (Hz) was obtained from the propeller-meter at each measurement point. The frequencies obtained on each day of experiments (and for each measurement point) were recorded and transferred to a spreadsheet on Microsoft Excel.

For converting these frequencies to velocities, a calibration chart was used. As this chart took the form of a linear plot, an equation was derived for ease of use. To do this, the chart was used to obtain 3 velocity values (on the horizontal axis) for 3 easily discernible frequency values (on the vertical axis). These values are show in Table 3 below.

Table 3 - Values obtained from Propellermeter Calibration Chart

Frequency (Hz)	Velocity (cm/s)
10	11.4
20	18.6
30	25.8

As the plot was linear, it was known that the equation would take the form of:

$$y = mx + c \tag{4}$$

Using this equation and the values shown in Table 3, *m* could be calculated as 1.389cm^{-1} and c could be calculated as -5.833Hz, giving the equation of conversion as:

$$y = 1.389x - 5.833 \tag{5}$$

Where y is the frequency measured by the propeller-meter (Hz) and x is the velocity (cm/s). As x was the unknown variable, the equation was rearranged to give:

$$x = \frac{(y + 5.833)}{1.389} \tag{6}$$

Implementing this equation into the same spreadsheet as the propeller-meter data enabled a quick conversion to obtain velocity values. The values from each day's measurements were then averaged to help identify outliers and give more certainty to the results. Various plots were then created to profile the velocities in various planes and help understand the behaviour of the flow within the tanks.

In some cases, particularly in the rectangular tank, the flow velocity was slower than could be detected by the propeller-meter, giving a reading of 0Hz. From the above conversion equation a reading of 0Hz would give a value of 4.2cm/s, but this cannot be assumed accurate at those points. What may be observed, however, is that at those points the velocity is not greater than 4.2cm/s.

3.4.3. Acoustic Doppler Data

From the experiments outlined in Section 3.3, the Acoustic Doppler recorded an array of data in 61 fields, which were then exported to MATLAB. These fields contained information on many aspects of data including: the distance from the probe to the bottom of the tank, the quality of the beams, the SNR ratios of the beams, the range of the measurements and the velocity profiles in the x, y and z directions (x always being in the direction of the horizontal flow).

The velocity profiles were provided in the form of a matrix, with each row of the matrix being a different time-step (each step being 0.01s) and each column being a different point in the measurement range (from 4cm from the base of the probe to 7cm, comprising of 1mm intervals). As the flow rates into both tanks were constant, time would did not affect the flow velocities, hence an average of the values at the different time-steps was calculated for each point within the measurement range.

Multiple different fields denoted the quality of the beams and readings from the acoustic Doppler, so a MATLAB script was created to compile these fields to achieve a high quality average velocity for each point on the range, with associated plots depicting velocity against depth. Fields of key interest for quality were the Profiles_SNRBeam fields and the Profiles_DataQuality Beam fields. These fields comprised of matrices with the same number of cells as the velocity profile matrices, with each cell corresponding to the equivalent cell in another field. For good quality data, the SNR beam values above 30 and Data Quality beam values of 0 were required. The MATLAB script was written so that if the SNR beam was above 30 or Data Quality equal to 0 then the corresponding velocity profile cell would be placed in a new matrix, and if not then that cell would be omitted from the new matrix. After this, the script was written so that the remaining time-steps were averaged resulting in a 1x30 matrix of average velocities for each point on the measurement range. Additionally, in the same script the mean bottom distance was determined, and the measurement range subtracted from this mean to give the distance from the base of the tank for each velocity value in the form of another 1x30 matrix.

This script was then run for the readings taken at each angle and the two 1x30 matrices were saved from each reading as the respective mean velocity and depth. A second script was then written to combine all depth and mean velocity readings for each angle and to plot them on a resulting scatter plot, with the potential of including the simulation and propeller-meter results on the same plot. Examples of these plots are displayed in Section 4.3.

To enhance the quality further of the Acoustic Doppler results, an algorithm could have been implemented into the first script, utilising the standard deviation and mean to detect and remove outliers and hence enhancing the data quality further. Due to time limitations, however, this was not achieved before the project deadline.

3.4.4. Blue Dye

Due to time limitations, quantitative analysis of the blue dye experimental results was not possible. However, qualitatively the observations made gave confidence in the symmetrical behaviour of the flow in the rectangular tank.

3.4.5. Error Analysis

Within all taken measurements there is some degree of error present. This may be due to a variety of reasons including: human reaction times, parallax errors with reading measurements and errors within the instruments used to take the measurements themselves. Errors can be either random or systematic, with random errors being randomly dispersed around the true value and systematic errors being a constant difference between the measured and true values.

Within this project, the majority of errors detailed are random errors, with the exception of the aforementioned error in filtration. Although the data collected with this error was replaced, the original error in masses was assumed to be systematic as the difference between the original masses of the filter papers and the masses after being washed and dried were approximately 0.001g. However, to some degree this was also a random error as this rectification did not solve all the issues.

The first way of mitigating error is repeating measurements and averaging these results, where possible. Over the course of the experiments at least 3 repeats of each data point were carried out, albeit over different days, and averages made of each reading. In the case of the Acoustic Doppler data, velocity data was collated over a period of time in one measurement and this also was averaged. The only exception to the three repeats was the final concentration data taken. Due to the array of errors including the initial filtration errors and also the slurry pump for the rectangular tank not adding the correct amount of OSP suspension, there was not enough time to take repeats before the project deadline.

Errors were also calculated for each measurement and these are displayed in Table 4 in Section 4.1.

3.5. Comparison and Validation Methodology

The validation aspect of the project covered two key areas: the comparison between the rectangular tank and the Swirl-Flo and the comparison between the CFD results and the experimental results. In addition to this a further validation of experimental results took the form of a comparison between the different forms of flow measurement: namely the propeller-meter and the Acoustic Doppler.

3.5.1. Flow Measurements

Both the propeller-meter and the Acoustic Doppler provided velocity profiles in the same location for 5 of the measurement points outlined in Section 3.3.1. This enabled a comparison of the two instruments as well as a validation of the experimental results generated by both in

different locations in the two tanks. The main form of comparison was carried out by calculating the percentage difference between the two measurements. This was calculated using the formula:

$$\Delta\% = \frac{x' - x}{x'} * 100$$

Where the x' is the larger value (velocity or other value) and x the smaller value (velocity or other value).

This comparison was additionally carried out between the mass flow rates with the mass flow rate values used instead of velocities and the results of which are displayed in Section 0 with the velocity differences displayed in Section 4.3.

3.5.2. Rectangular Tank Vs Swirl-Flo

The two tanks studied were compared using the collected experimental data. The key measurements used for comparison were the concentration measurements. These measurements enabled the capture efficiency to be calculated for each tank, which enabled a comparison of the performance of each tank. This efficiency details the percentage of the OSP that is retained within the tank and underflow and was calculated by the following formula:

$$CE = \frac{(m_i - m_o)}{m_i} * 100 \quad (8)$$

Where CE is the capture efficiency (%), m_i is the mass flow rate (g/s) at the inlet and m_o is the mass flow rate (g/s) at the overflow.

This efficiency was expected to be around 60% as a standard for all primary sedimentation tanks [5]. In addition to this the time it took to achieve a steady-state concentration was also considered in terms of performance, although in industry as these tanks are continually run this is not as important as the capture efficiency. The time to steady-state concentration can be identified from the concentration plots displayed in Section 0, as the time at which convergence is achieved.

The velocity profiles measured in the tanks were used to compare the internal behaviour of the tanks, however the most important factor for comparison between tanks is in the collection efficiency or outflow concentrations.

3.5.3. CFD Results Vs Experimental Results

The key area for comparison was between the CFD and experimental results. This was key for validating the CFD model created by the simulation team and giving confidence in any further results generated. Data from the simulations was collected and provided by Russell [18] and Bentley [19].

Both the concentration results and velocity measurements collected from experiments were used for this validation. From the concentration results, the time to achieve steady-state could be compared, as the simulations stated the time it took to converge. This could be compared to the time at which convergence occurred on the experimental plots. Furthermore, the mass flow rate after convergence could be compared, using the same percentage difference equation shown earlier, however instead of velocity values, the mass flow rate values were used. The concentration comparison plots are displayed in Section 4.5.1.

The velocity measurements were also used to compare the modelled behaviour within the tank to the observed behaviour. This comparison was carried out by creating velocity profiles for the same point and comparing the CFD values and the experimental values. These plots display the depth on the y-axis instead of the x-axis to enable easy understanding of the behaviour within the tanks and can be found in Section 4.5.2.

3.6. Health and Safety Considerations

As with all experimental procedures, consideration of health and safety is a prerequisite. For the experiments outlined, many health and safety aspects needed to be considered. The key of these being: flooding the building, electrical appliances coming into contact with water, the use of a drying/curing oven and consideration of the hazards associated with OSP and glue. This entailed risk assessments being drawn up, highlighting the potential risks and outlining steps for mitigating these risks, which were duly completed and copies supplied to the laboratory technicians before commencing any of the experiments. These health and safety issues are further expounded on in Section 6.2.

A further consideration during experiments was the use of water. The experiments outlined required access to a large amount of water at a large flow rate. This resulted in planning experiments so that there was enough time for the tank the water was drawn from to fill up again, it also resulted in a requirement of efficiency with taking measurements and due to the limitations meant planning repeats over days rather than in one experiment. Additionally, with the large water intake came a need to consider the disposal of a large volume of water. This resulted in an agreement with South-West Water for the disposal of up to 20,000L of

water containing OSP a day. This further consolidated the need to repeat the experiments over days. These sustainability issues are further expounded on in Section 6.3.

3.7. Problems encountered

Over the course of the project various problems were encountered. The first of these came in the form of the need to redesign the rectangular tank. The rectangular tank used for experiments was not built as a wastewater separation tank: It was designed to accommodate flows of a vastly smaller magnitude than the Swirl-Flo® tank, or equivalent rectangular tanks used in industry. This meant that the efficiency of the tank was greater than the industry standard, with a slow flow rate being a key contributor to this efficiency. The efficiency of the tank could be reduced through either altering the dimensions of the tank or increasing the flow rates into and out of the tank.

The tank originally could only accommodate a flow rate of 8L/min into the tank and any attempt to increase that flow rate was hindered by the dimensions of the pipes for the outflows. Furthermore it was found that altering the depth of the tank had no effect on the efficiency, leaving the only possible dimension modifications being the width and length. A ratio was also found denoting the standard ratio between length and width of a rectangular tank as 4:1. Calculations involving a selection of equations and this ratio were implemented in Microsoft Excel and utilising the goal seek function the ideal dimensions were found to be 26cmx6cm for the tank at a flow rate of 8L/min. As a group it was decided that it would not be practical to carry out such extreme modifications, so it was decided to remove the original overflow pipe and replace it with a pipe of a larger diameter which enabled an inflow flow rate of over 24L/min. Further to this work was carried out by Wye [20] to elevate the base of the tank, reducing the hydraulic retention time. Although this did not directly affect the efficiency, it reduced the time the water was present in the tank. In addition to the elevation of the base, a hopper was also designed by Wye [20] which gave the base an incline to aid the removal of the sludge bed. These design modifications suitably reduced the efficiency of the tank although this was still not identical to those used in industry.

A final problem that was encountered involved the simulations and the servers that ran them. These servers were repeatedly down over the course of the project, causing delays in producing simulation results. Furthermore, the run time for the simulation of the Swirl-Flo® exceeded the deadline for the project, meaning that converged results could not be obtained. Despite this some data was obtained, although some inaccuracies were present. Regardless of this, the same method of analysis that would have been carried out on the completed simulation results was used on these results and comparisons made to the experimental data.

4. Presentation of Experimental and Analytical Results

This section presents results and findings from the experiments and analysis detailed in the previous sections in the form of relevant graphs and tables.

4.1. Error Analysis

As detailed in Section 3.4.5, some degree of error is present in all measurements taken. Section 3.4.5 also details methods of calculating errors, and Table 4 displays the measurement types with their respective errors. For some quantities, the error varies between values and hence the average of the errors is stated, although in later figures the error bars are specific to each individual value.

Table 4 - Table of Absolute and Relative Errors for Values within the Project

Measurement	Absolute Error	Relative Error
Flow rates		
Rectangular Tank Inflow (L/s)	±0.0025L/s	±0.0065
Rectangular Tank Overflow (L/s)	±0.0042L/s	±0.011
Rectangular Tank Underflow (L/s)	±0.0017L/s	±0.078
Swirl-Flo® Tank Inflow (L/s)	±0.267L/s	±0.33
Swirl-Flo® Tank Overflow (L/s)	±0.18L/s	±0.26
Swirl-Flo® Tank Underflow (L/s)	±0.046L/s	±0.38
Concentration Calculations		
Mass of paper (g)	±0.0005g	±0.0006
Sample mass (g)	±0.001g	±0.043
Sample Volume (mL)	±5mL	±0.018
Sample time (s)	±5s	±0.083
Mass Flow Rates		
Swirl-Flo® Overflow (g/s)	±0.018g/s	±0.3
Swirl-Flo® Underflow (g/s)	±0.008g/s	±0.4
Rectangular Tank Overflow (g/s)	±0.0025g/s	±0.05
Rectangular Tank Underflow (g/s)	±0.0007g/s	±0.14
Velocity Profiles		
Depth (m)	±0.01m	±0.12
Propellermeter Velocity (cm/s)	±1.5% [21]	
Acoustic Doppler Velocity (m/s)	±0.001m/s [22]	

The relative errors provide an idea of the comparison between the error and the size of the measured quantity. From Table 4 it can be seen that all the relative errors are less than 0.5, with the greatest relative error being for the Swirl-Flo® Underflow mass flow rate and the

smallest relative error being for the mass of paper for the concentration calculations. The larger relative errors are for values which were calculated using other measurements present, which cause a summation of relative and absolute errors. Even then, these values are so small as to be insignificant compared to the values they affect.

4.2. Steady-State Concentration

From the experiments and methodologies outlined in Sections 3.2 and 3.4.1, plots for both tanks were created depicting concentration against time during the experiments. As previously stated, these concentrations were also converted into the volume fraction of the OSP (alpha) and the mass flow rate (g/s). Both the alpha and mass flow rate plots displayed the same trend. The mass flow rate plots are displayed in this section for comparison with the CFD results further down.

4.2.1. Rectangular Tank Results

Figure 1 displays the dispersed-phase mass flow rates for overflow and underflow in the rectangular tank.

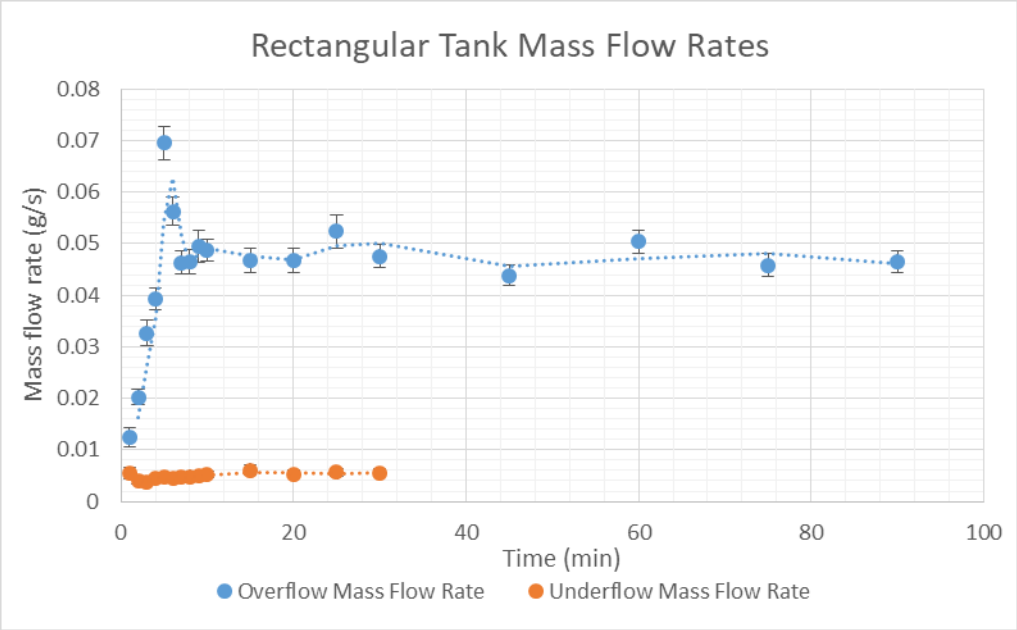

Figure 1 - The Empirical Rectangular Tank Mass Flow Rates

From this figure, it may be observed that the concentration achieves steady state 8 minutes into the experiment for both underflow and overflow. The overflow converges to a mass flow rate of 0.05±0.0025g/s, while the underflow converges to a mass flow rate of 0.005±0.0007g/s. It may be noted that the underflow mass flow rate is 90% smaller than the overflow mass flow rate. This is initially surprising as the underflow typically has a larger concentration of OSP than the overflow. However, the mass flow rate is calculated by

multiplying the concentration by the flow rate, and as the underflow has a flow rate of 1.3L/min (94% smaller than the overflow), the underflow has a proportionately smaller mass flow rate. The mass flow rate values are quoted to 1 significant figure due to the small fluctuations observed in Figure 1.

Error bars denoting the absolute errors for each value were plotted, however for the underflow mass flow rate the vertical bars were too small to be visible. Similarly, for both the overflow and underflow the horizontal error bars are too small to be visible. A moving average trend line was plotted on all mass flow rate plots to enable clearer identification of convergence.

4.2.2. Swirl-Flo® Results

Figure 2 displays the dispersed-phase mass flow rates at the underflow and overflow for the Swirl-Flo®.

From this figure, it may be observed that steady-state concentration was achieved 5 minutes into the experiment. The underflow converges to 0.02±0.008g/s while the overflow converges to 0.06±0.018g/s and the percentage difference between the underflow and overflow mass flow rates is 66.7%. This is a smaller difference than the equivalent values for the rectangular tank, but again the underflow mass flow rate is smaller due to the lower flow rate. 30 minutes into the experiment an anomaly was identified in the overflow mass flow rate as this value is vastly larger than any others displayed. Furthermore, the overflow mass flow rate fluctuates around 0.06g/s, however this value falls within the range of error for all points.

Again, error bars denoting the absolute error for each value were plotted vertically, however horizontally the error was indistinguishable.

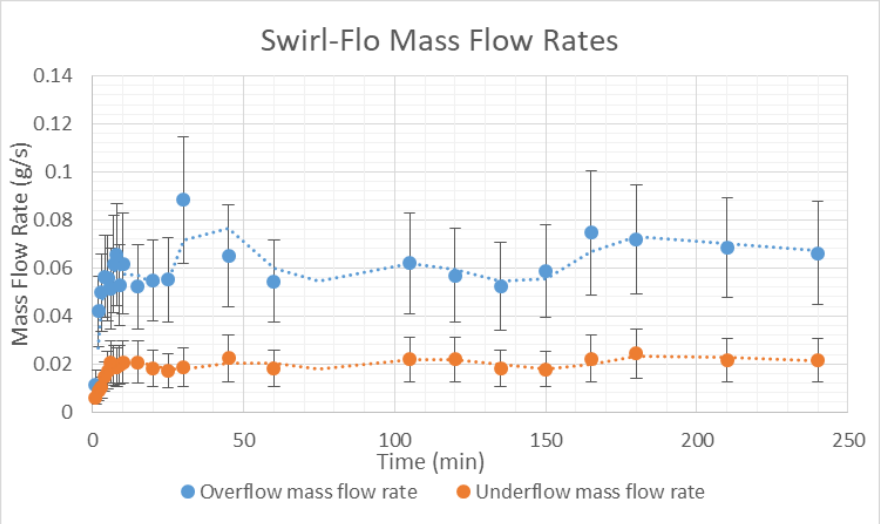

Figure 2 - The Empirical Swirl-Flo® Mass Flow Rates

4.3. Flow Velocities

From the velocities collected through the processes outlined in Sections 3.3 and 3.4 various plots were created a selection of which are presented within this section. The plots presented display velocities measured by both the Acoustic Doppler and the propeller-meter for comparison and evaluation of both in Section 4.3.3.

4.3.1. Rectangular Tank Empirical Velocities

For analysis of the rectangular tank, the propeller-meter data was utilised to create various plots depicting the velocity profiles viewed from different directions. The direction utilised for most velocity profiles displayed in this report is a velocity-depth plot for a single stated location within a tank. Other plots created, however, observed the change in the velocity profile across the length of the tank for a given width or across the width of the tank for a given length.

Figure 3 displays the velocity profile change with the length of the tank at a 55mm depth, where 0mm is at the inlet weir. The velocity magnitudes were observed to be largest at the inlet weir and were seen to decrease in magnitude along the length of the tank. As explained in Section 3.4.2, the velocity values of 4.2cm/s were calculated from a reading of 0Hz, implying the velocities at these points may be any value below 4.2cm/s.

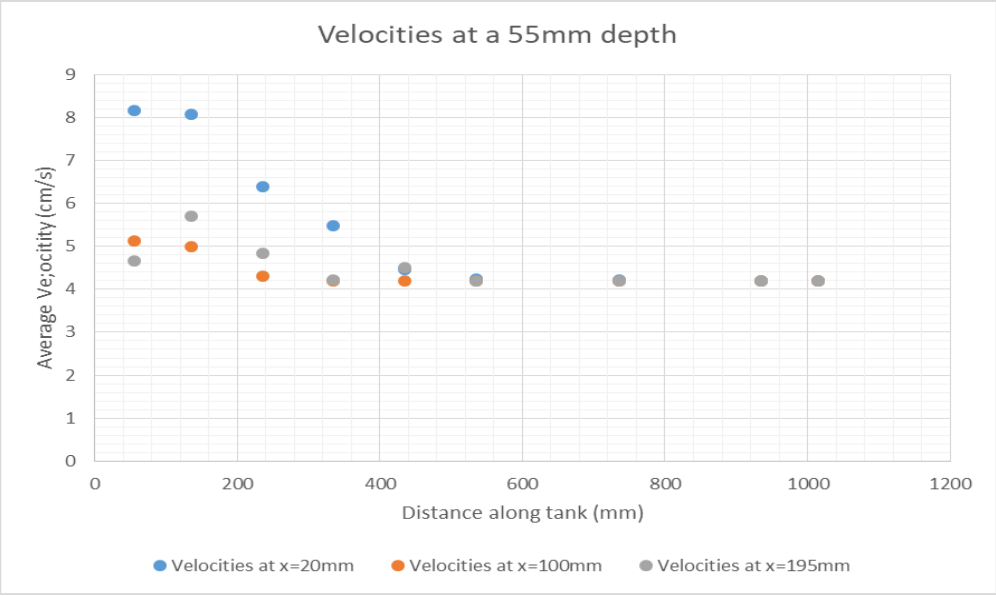

Figure 3 - Propeller-meter velocity profile along the length of the rectangular tank at a 55mm depth

Of interest, from Figure 3, the variation in behaviour at 3 separate points across the width was observed, with measurements referenced from the tank edge and 195mm is near the centre of its width. From this data it may be observed that the average velocity was greatest

near the edge of the tank closest to the inlet weir. To the other two widths which displayed similar but lower behaviours, potentially due to interactions of the flow with the Perspex tank walls. However, in comparisons with the simulation and Acoustic Doppler results (expounded in Section 4.5.2.1) this larger value was seen to be vastly different to the other measured values, calling into question the reliability of the propeller-meter when measuring low flow velocities.

Comparative plots between Acoustic Doppler and propeller-meter values are shown in Figure 4, with similar plots comprising of simulation results displayed in Section 4.5.2.1,

From Figure 4, the differences between the propeller-meter and Acoustic Doppler results may be seen, particularly regarding their magnitude. For both (a) and (b), the propeller-meter recorded vastly larger velocities than that by the Acoustic Doppler, further shown in Section

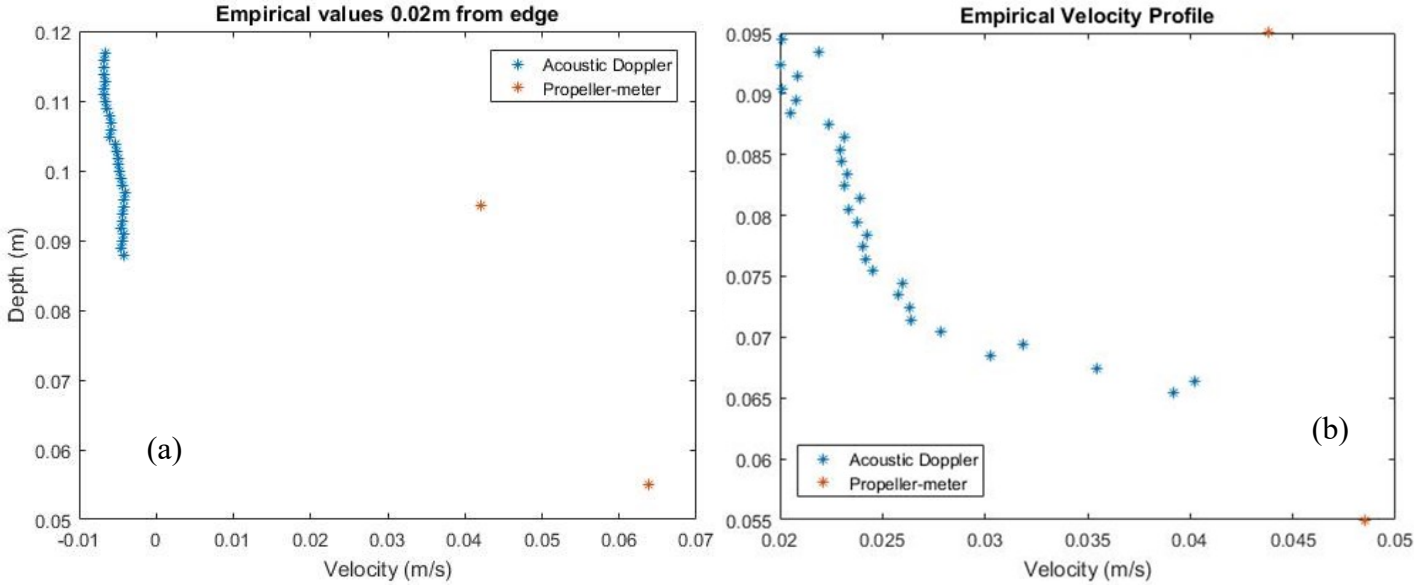

Figure 4 - Acoustic Doppler and propeller-meter velocity profiles 0.235m from the inlet weir at (a) x=0.02m and (b) x=0.195m from the tank edge.

4.5.2.1 in comparison with simulation results. However, the trend of decreased velocity with increased depth was observed for both the propeller-meter and Acoustic Doppler results.

4.3.2. Swirl-Flo® Empirical Velocities

Similar analysis utilising flow velocity measurements was carried out on the Swirl-Flo®. A variety of plots were created using the propeller-meter data depicting the velocity profiles from different views. These plots included: scatter plots of velocities against depth at each of the different measurement angles and radii, scatter plots and radar plots of velocities against angle at each of the depths for the corresponding radii (the radar plots enabled a clearer picture of the behaviour within the Swirl-Flo® compared to the scatter plots) and horizontal

bar charts which enabled a clearer plot of velocities against depth for each radial location. The depths of the measurements were measure from the measurement jig, 71mm above the water surface.

Figure 5 is a radar plot created to show the variation in velocities measured by the propeller-meter at a depth of 0.29m. While this plot does not depict the full 360º of the Swirl-Flo®, it still provides insight into the velocity profiles in relation to the Swirl-Flo® shape. Through this plot and others like it, it may be observed that the velocities are always larger closer to the walls of the Swirl-Flo®, with smaller velocities closer to the centre. Furthermore, from Figure 5 it may be easily identified where the velocities are largest and smallest. In the experiments, the water entered the Swirl-Flo® through an inlet situated between 218º and 313º. Knowing this, it was observed that the velocities are greatest in the opposite third of the tank to the inlet, and smallest just before the inlet. The smallest velocities before the inlet were due to a deflector plate directing the inflow, resulting in a spot within the tank between 228º and 313º where the flow is lessened.

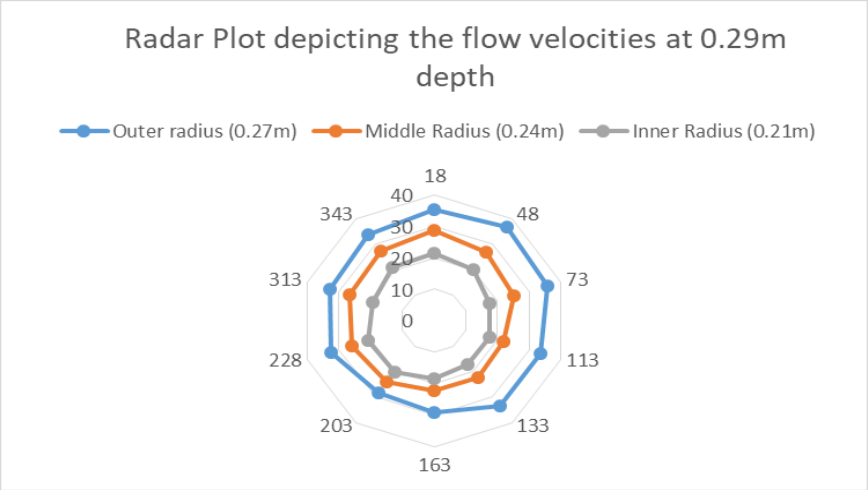

Figure 5 - A radar plot depicting the variation in velocities at a depth of 0.29m

Figure 6 depicts velocities for each of the three radii against depth at 313º. This enables a clear understanding and easy observation of the comparative proportions of velocity between depths and radii.

This figure again shows that the flow closer to the walls of the Swirl-Flo® is greater than that closer to the centre, as by the time the flow reaches the centre it has lost its initial momentum. Additionally, as this plot depicts the values at 313º, it also exemplifies the earlier observation of smaller flow velocities just before the inlet, with the inner value particularly displaying a velocity of 6cm/s, vastly smaller than the other measured velocities.

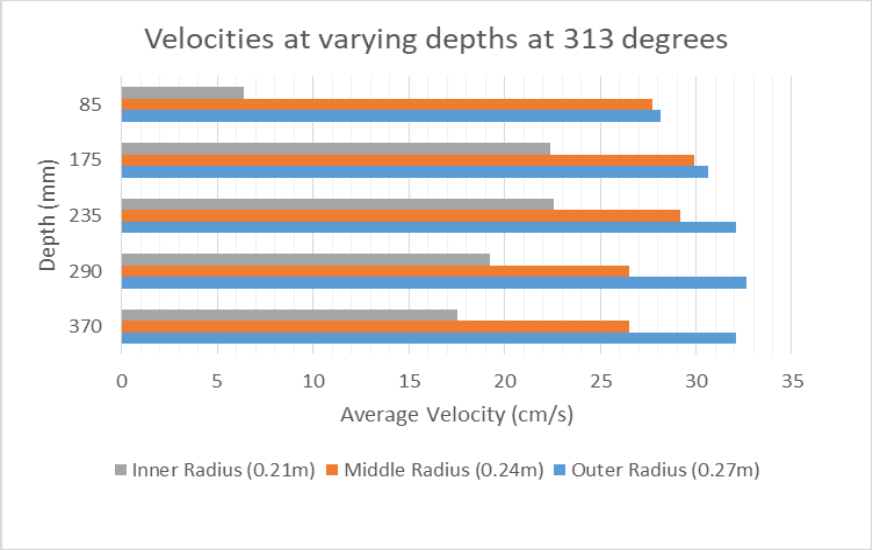

Figure 6 - A horizontal bar chart depicting propeller-meter velocities at 313º

Figure 7 shows the Acoustic Doppler and propeller-meter profiles at 48º and 203º, similar

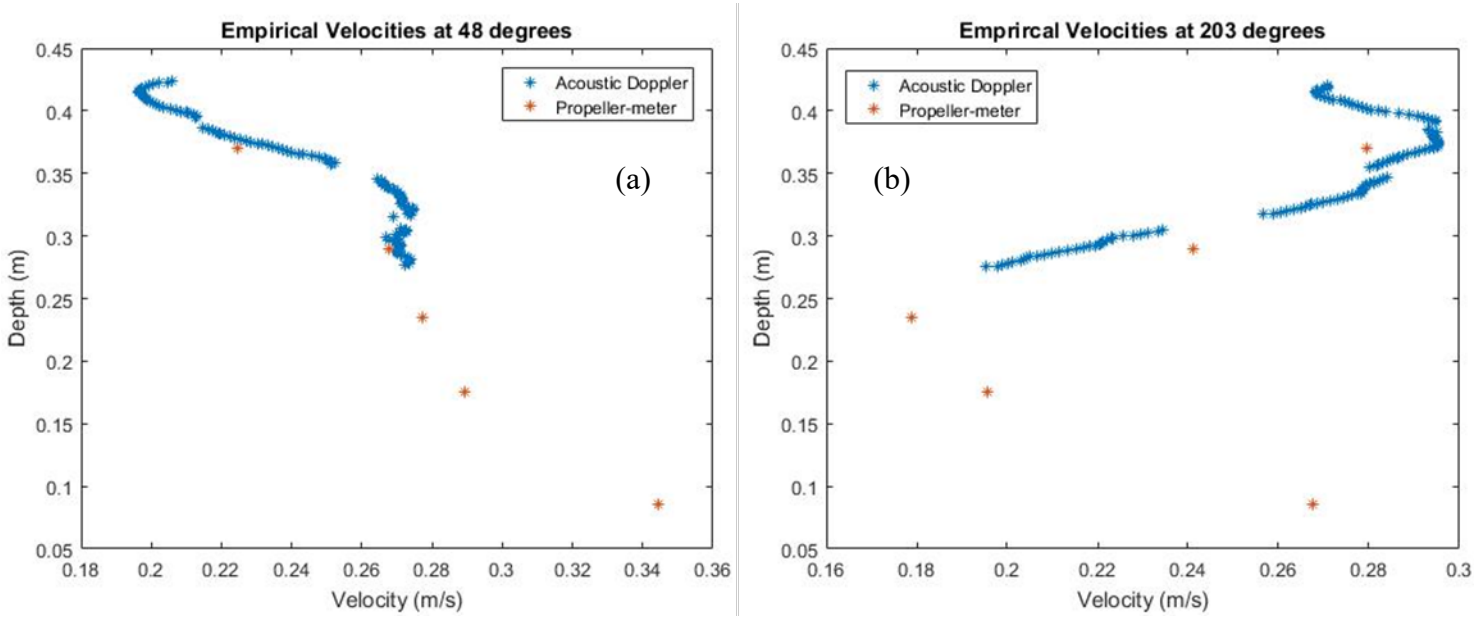

Figure 7 - Acoustic Doppler and propeller-meter velocity profiles at (a) 48o and (b) 203o

plots with the addition of the simulation data are shown in Figure 11.

These two plots depict the variation in velocities with relation to angle, as at 48º the velocity profile decreased with depth while at 203º the velocity profile increased to a peak magnitude and then starts to decrease again. It is also noted that from all the plots and figures shown regarding empirical velocities for the Swirl-Flo, none exceed 0.35m/s (35cm/s).

4.3.3. Flow Measurement Comparison

From the results detailed above regarding the Acoustic Doppler and propeller-meter in the two tanks, several key observations can be made. Of key importance was the high uncertainty in the results of the propeller-meter where the velocities are low, as this can lower confidence in the results given. This also meant the versatility of this instrument was reduced. However, where velocities are in the correct range for the propeller-meter to take measurements, there was great confidence in the results. In the case of this project, when utilised in the Swirl-Flo®, the Acoustic Doppler and propeller-meter results (shown in Figure 7) were very similar, providing great confidence in the accuracy of the results.

Compared to the Acoustic Doppler, the propeller-meter did not provide as much information, however in the case of this project it provided as much as was needed and was thus efficient to use, again demonstrated by the variety of measurements it was used to take. On the other hand, the Acoustic Doppler recorded many different fields of information, and many of these were useful for determining factors such as the data quality and the distance to the base of the tank as well as a variety of different velocity profiles. However, comparing the number of data fields recorded compared with those that were used for analysis and results applicable to this project, it could be argued that it was not as efficient as the propeller-meter, further shown by the smaller number of measurements it was used to take.

Both the Acoustic Doppler and propeller-meter had advantages and disadvantages when utilised within the project, however combing the information gained from both results gave greater confidence in the experimental results obtained and comparisons made with the simulation results.

4.4. Sedimentation Tank Comparison

Through the experiments carried out and results obtained, several observations and comparisons were made. Regarding the initial set-up of each tank, the Swirl-Flo® is designed to function with a high flow rate passing through the tank, while the rectangular tank and other equivalent sedimentation tanks are designed to reduce the flow rate to increase the quantity of suspended particles that settle out. However, due to the Swirl-Flo® utilising vortex separation, the higher flow rate does not impede the removal of suspended particles.

In terms of capture efficiency, the Swirl-Flo® had inflow and (converged) overflow mass flow rates of 0.24g/s and 0.06g/s respectively. This gave a 75% capture efficiency for the Swirl-Flo®. The rectangular tank had inflow and overflow mass flow rates of 0.12g/s and 0.05g/s respectively. This gave a 59% capture efficiency for the rectangular tank. The percentage difference between capture efficiencies is 21.3%. The larger capture efficiency for

the Swirl-Flo® meant it retains a larger proportion of the OSP than the rectangular tank although this percentage is higher than the industry standard while the rectangular tank efficiency is similar to the industry standard of 60%.

Furthermore, from velocity profiles within the tanks, it is observed that the rectangular tank has vastly smaller flow velocities compared to the Swirl-Flo®. This difference is not necessarily a negative as most sedimentation tanks require small flow velocities to efficiently work. However, within wastewater processing, there is an advantage to being able to utilise a higher flow rate within the primary stage as it reduces the need to implement measures to reduce this flow and enables faster processing.

4.5. Experimental and CFD Comparison

This section details the comparison between the simulation and experimental results, utilising various plots of mass flow rates (for steady-state concentration comparison) and velocity profiles. As previously stated the simulation data for the rectangular tank and Swirl-Flo® were provided by Bentley [19] and Russell [18] respectively.

4.5.1. Concentration Comparison

Figures 8 and 9 display comparative plots of simulation and experimental overflow and underflow mass flow rates for the rectangular tank and Swirl-Flo® respectively.

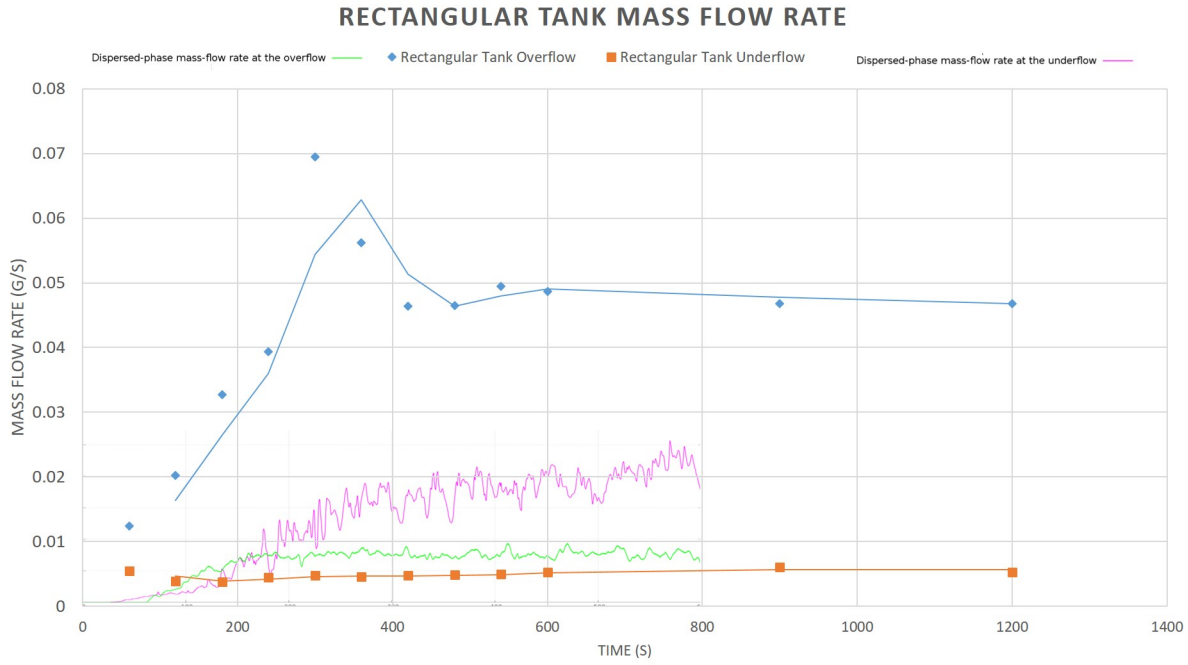

Figure 8 - Empirical and Simulation Overflow and Underflow Mass Flow Rates in the Rectangular Tank

From Figure 8, it may be seen that the simulation and experimental results display similar trends in behaviour over time, with convergence occurring for both underflow and overflow mass flow rates by 480 seconds (or 8 minutes). A key difference however, was that the simulation overflow mass flow rate is smaller than the underflow mass flow rate while the experimental results are the opposite with a larger overflow mass flow rate. One further difference was that the experimental overflow mass flow rate is sufficiently larger than both simulation mass flow rates. There was an 84% difference between the overflow mass flow rates (taking the simulation overflow convergence to be approximately 0.08g/s), and a 75% difference between the underflow mass flow rates, (taking the simulation underflow convergence to be approximately 0.02g/s). The reason for the large differences between experimental and simulation results is likely due to an error within the settling velocity model.

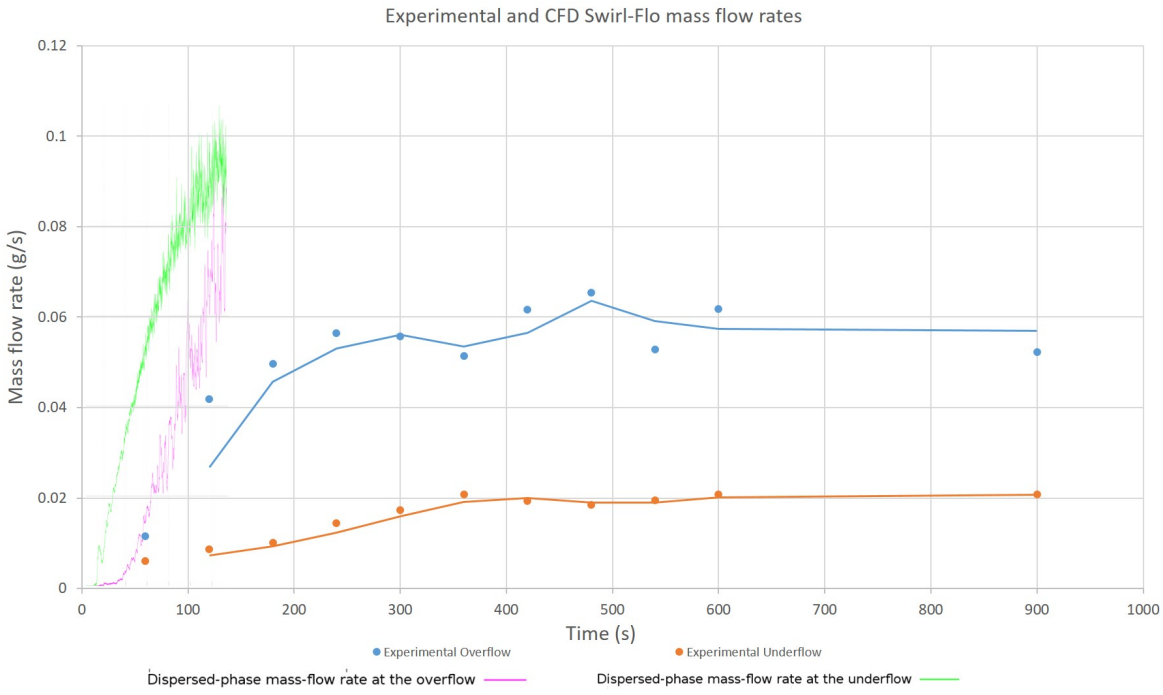

Figure 9 - Empirical and Simulation Mass Flow Rates for the Swirl-Flo®

From Figure 9 a mathematical comparison between the simulation and experimental converged results could not be obtained. This was because there was not enough computational time to run the Swirl-Flo® simulation to completion before the project deadline (the full simulation projected to take as much as 3 months). In the time available the simulation was run for a 135s experimental time, within which experimental mass-flow rate convergence was not achieved. Information on simulation overflow and underflow mass flow rate convergence cannot be inferred beyond the observation that at 135s the simulation appears to be diverging, not converging. However, within the initial 135s, both of the overflow mass flow rates exhibit a similar gradient. It can be observed that both simulation

mass flow rates appear set to converge with higher mass flow rates than those measured by the experimental studies.

4.5.2. Velocity Profile Comparison

This subsection details the comparison of the velocity profiles within the two tanks through various plots depicting the profiles generated by the simulation, Acoustic Doppler and propeller-meter results. As this section solely looks at the comparisons between simulation and experimental data, the velocity profiles were split into sections for each tank for clarity.

4.5.2.1. Rectangular Tank Velocity Profiles

Figure 10 displays the velocity profiles for the rectangular tank comparing the simulation velocity profile with that measured by the Acoustic Doppler and propeller-meter. Figure 10(a) displays the profile 0.02m from the edge of the tank (the x-direction being the width) and 0.055m down the length of the tank (from the inlet weir), while Figure 10(b) is the same distance from the inlet weir but 0.195m from the tank edge, near the centre of the tank width.

In Figure 10(b), the simulation and Acoustic Doppler results yielded negative velocities. This may be due to location of the measurement point within the tank, as further velocities measured by the Acoustic Doppler at similar width locations (an example shown in Figure 4(a)) also yielded negative velocities. In this location, the flow was likely to be interacting with the Perspex tank wall resulting in potentially negative flow.

While in both (a) and (b), there was a difference between the magnitudes of the Acoustic Doppler and simulation results, this difference was typically in the region of 0.01m/s and was a smaller difference than that between these results and the propeller-meter results. The reason for this large difference in the propeller-meter results was in part due to the insensitivity of the propeller-meter to low flow velocities. While results were obtained by the propeller-meter, due to the low flow, the propeller rotated at a very low frequency with the potential for incomplete rotations within the time period for frequency calculation. Moreover, it was observed within experiments that readings occasionally fluctuated between 0 and the value recorded.

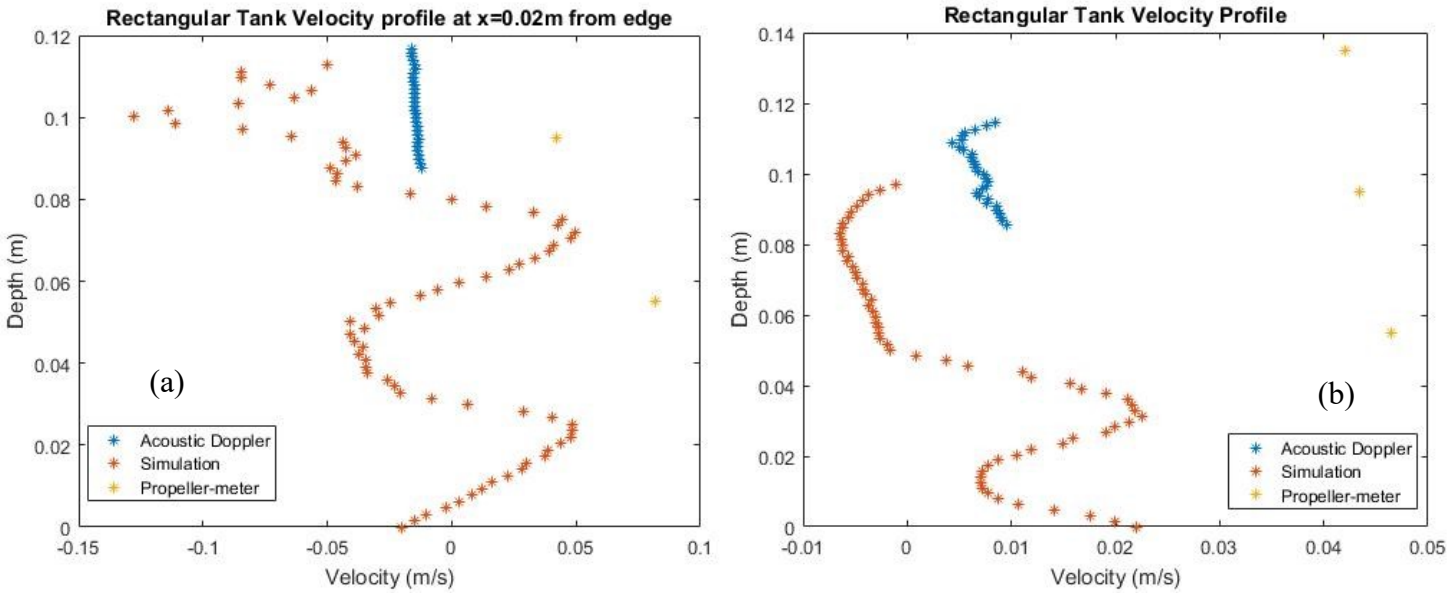

Figure 10 - Acoustic Doppler, simulation and propeller-meter velocity profiles 0.055m from the inlet weir for (a) x=0.02m and (b) x=0.195m from the tank edge

One further observation from (b), was the similar trend between the simulation and Acoustic Doppler data despite the magnitude difference. This suggests that the behaviour within the simulation is comparable to the experimental behaviour. The magnitude difference may well be caused by inaccuracy in the simulation boundary conditions.

4.5.2.2. Swirl-Flo® Velocity Profiles

Figure 11 displays a selection of the Swirl-Flo® velocity profiles at various points in the Swirl-Flo®. At the different angles, the variation between velocity magnitudes and depth was observed. In particular, the Acoustic Doppler and propeller-meter profiles are very similar at 18º and 48º with velocity typically decreasing as the depth increased. However, at 113º the velocity increased with depth. At 203º the velocity profile is different to increase with depth to a peak value at approximately 0.38m and then decreased with depth after that. As the velocity profiles measured by the Acoustic Doppler and propeller-meter are similar in magnitude and trend, this gives confidence in the profiles portrayed by the empirical results.

However, at 113º the velocity increased with depth. At 203º the velocity profile is different to increase with depth to a peak value at approximately 0.38m and then decreased with depth after that. As the velocity profiles measured by the Acoustic Doppler and propeller-meter are similar in magnitude and trend, this gives confidence in the profiles portrayed by the empirical results

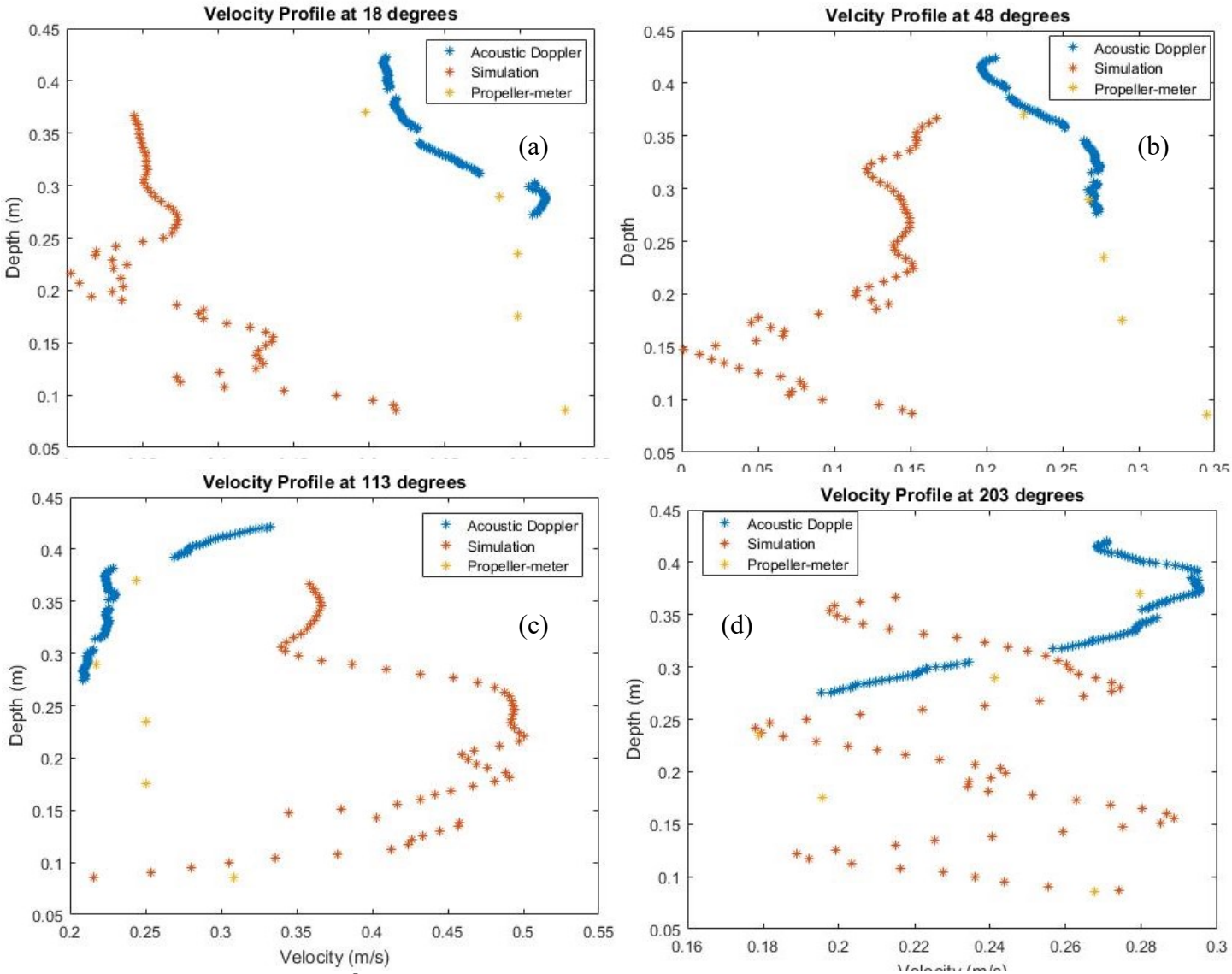

Figure 11 - Swirl-Flo® Empirical and Simulation Velocity Profiles at varying polar coordinate angles

While the magnitudes were different between the simulation and empirical results, the simulations appear to emulate a similar shaped profile to the empirical data. This is particularly noticeable in Figure 11(a) and Figure 11(d). In these figures, the Acoustic Doppler and simulation profiles both exhibit similar behaviour through peaks in magnitudes and the gradients of the changes in velocity with depth. This suggests that while the simulation magnitudes were different, the simulations portray similar flow behaviour within the tank to that observed. This difference in simulation magnitudes may be due to an error within the modelling conditions, such as boundary conditions, mesh size or simulation runtime.

4.6. Validation

The goal of validation was to utilise the comparative plots created using the results from the simulations and empirical studies to provide confidence in the simulation results. Displayed in Section 4.5 are the various plots created for this comparison, obtained for velocity profiles and dispersed-phase mass flow rates (equivalent to steady-state concentration).

From the dispersed-phase mass flow rate plots it was observed that the rectangular tank simulations and empirical studies both obtained convergence within 8 minutes, although there was a large discrepancy between the mass flow rates for the outflow of both. Additionally, the Swirl-Flo® could not be run long enough to achieve completion.

From the velocity profiles, for the rectangular tank, there was some discrepancy between the Acoustic Doppler and propeller-meter empirical values. Although, the Acoustic Doppler produced values in the same region as the simulation data. For the Swirl-Flo® velocity profiles, the Acoustic Doppler and propeller-meter empirical values validated each other but were of a different magnitude to the simulation results. This may be due to the simulation not being run to completion. However, the simulation data and Acoustic Doppler values did display similar trends.

Qualitatively, the similarities between trends, and the convergence times, leads to the conclusion that the simulations show the same observed behaviours as the experiments, barring some numerical offset. However, numerical data cannot be easily discounted and quantitative analysis using percentage error was required. From this analysis, it was found (and detailed in Section 4.5.1) that there was an 84% difference between the simulation and empirical overflow mass flow rates for the rectangular tank and a 75% difference in mass flow rates for the underflow of the same tank. These differences between the empirical and simulation velocities varied between tank and location meaning the percentage differences varied between 0.2% and 58% for the Swirl-Flo® and 12% and 56% for the rectangular tank. This implies that due to the large differences, confidence cannot be given to the numerical results of the Swirl-Flo® simulations. Running these to completion, however, may solve this issue as this may provide a greater insight in comparison. These percentage differences may, as before, be due to errors in the simulation boundary conditions.

5. Discussion and conclusions

Over the course of the project many things were observed and learnt, particularly through the empirical studies carried out on both tanks and the analysis and comparison of the data obtained from these and the simulations.

5.1. Experimental Findings

From the experiments carried out on both the Swirl-Flo® and the rectangular tank, the flow behaviour with regards to velocity within each tank was observed. Within the rectangular tank, it was observed that the flow velocities were larger closer to and decreased with distance from the inlet weir. Similarly, with the Swirl-Flo®, it was observed that the velocities increased with the distance from the centre of the tank, furthermore it was observed that the velocities were greatest the other side of the tank to the inlet and smallest in the shadow of the inlet pipe due to the deflector shield.

Comparatively, it was observed that the velocities present in the Swirl-Flo® were larger than those present in the rectangular tank. This exemplifies the key difference in how the tanks function: the rectangular tank reduces the flow rate to enable the suspended particles to settle, while the Swirl-Flo® uses the large velocity and the generated vortex to aid the settling of the suspended particles.

Additionally, from the experiments, the concentration at the overflow and underflow outflows was calculated from sample filtration. This was converted to dispersed phase mass flow rates and plots of which were used to determine steady-state concentrations from the convergence of values. From these, it was found that the rectangular tank converged in 8 minutes, with overflow and underflow mass flow rates of 0.05±0.025g/s and 0.005±0.0007g/s respectively. Similarly, it was found that the Swirl-Flo® converged in 5 minutes, with overflow and underflow mass rates of 0.06±0.018g/s and 0.02±0.008g/s. This gave a 16.7% and a 75% difference between the mass flow rates for the different tank overflows and underflows respectively. It was observed that the mass flow rates at the overflow were significantly larger than the underflow, which was unexpected due to the larger concentration present in the underflow samples. This was found to be due the size of the flow rates at the outflows: the underflow flow rates were vastly smaller than the flow rates at the overflows

Capture efficiencies were calculated from the experimental data for both tanks, with the Swirl-Flo and rectangular tanks having respective 75% and 59% capture efficiencies. These efficiencies depict the proportion of olivestone powder removed by the tank from the overflow.

A key area of analysis was in the comparison between provided simulation results and the collected empirical data which comprised of comparative plots of mass flow rates and velocity profiles. From these plots it was observed that the simulation of the rectangular tank converged in the same time frame as the experiments, however the mass flow rates were of different magnitudes, which could be due to an inaccurate settling velocity model for OSP. Similarly, the velocity profiles of points in the Swirl-Flo® displayed a difference in

magnitudes between the simulation and empirical results, however in some cases similar trends within the different data sets could be observed. The differences in velocity magnitudes could be due to the Swirl-Flo® not being run to completion.

5.2. Analytical Significance

All the findings and observations described have significance to this project and the larger group project deliverables. Of particular significance is the comparison between the simulation and empirical results. As stated none of the equivalent results generated by the simulations and empirical studies matched, although similar behavioural trends were noticed. However, with large percentage errors varying from 12% to 84% calculated for various velocity values, the simulations are not empirically validated.

Another area of particular significance is the comparison between the two sedimentation tanks. As stated, the velocity profiles within each tank varied greatly, with the rectangular tank velocities being smaller in magnitude than those in the Swirl-Flo®. This clearly shows the difference in how the tanks operate, however, from the overflow percentage differences it can be seen that a similar mass flow rate is achieved at the overflow. Furthermore, the capture efficiencies calculated show that the Swirl-Flo® has a greater capture efficiency than the rectangular tank, (75% and 59% respectively). This means that compared to the industry standard (for primary sedimentation tanks) of 60%, approximately the efficiency of the rectangular tank, the Swirl-Flo® performs better regarding the removal of suspended particles.

5.3. Observations for Future Work

There are a few areas in which work can be carried out to extend the project. Within this project, the addition of blue dye to the tanks was used to gain a qualitative understanding of the flow behaviour, however time restraints meant that further investigation into gaining quantitative values was not achieved. This means that an area of future work is to investigate how added blue dye could be used to obtain quantitative information on the flow profile, potentially through using a software such as ERDAS IMAGINE [20].

Additionally, the Acoustic Doppler provided many fields of data denoting different aspects of the readings from velocity profiles to data quality. Within this project, tangential velocities within the Swirl-Flo® were the focus for comparison. However vertical and radial velocities were also measured by the Acoustic Doppler and were obtainable from simulation results, these could form a new area of investigation, validation and comparison between empirical and simulation results.

Finally, with completed simulation results (with correct boundary conditions), it would be possible to validate the simulations using the empirical data with greater confidence.

5.4. Concluding Points

The overall findings of the project may be summarised in the following points:

- The Swirl-Flo® design enables the use of a vortex to separate particles at a greater velocity which results in a greater capture efficiency compared to the rectangular tank
- Similar behavioural trends in steady-state concentration convergence and velocity profiles are observed for both the empirical and simulation results for both the Swirl-Flo® and the rectangular tank.
- The magnitudes of the values generated by the simulation and empirical results have a large percentage difference so the simulations are not empirically validated.

6. Project management

Within a group project of this size and scope, management was key for the accomplishment of objectives. Furthermore, the interdependence between work packages and individual projects resulted in an awareness of a timeline for different deliverables to be achieved by. This guided the management procedures and systems that managed this project which are detailed in this section. Additionally, sustainability and health and safety considerations are touched on as in Section 3.6.

6.1. Management Procedures and Systems

Similarly to the management system for the group outlined in the Group Report [24], the project outlined in this report required management. The management of the group as a whole entailed a detailed management spreadsheet created and maintained by the project manager, Wye [20]. This outlined the deliverables for the group project and which group members were to achieve them along with a Gantt chart and workflow flow chart which stated the deadlines for different deliverables to be achieved by. In addition, a formal weekly meeting with the project supervisor, Dr Gavin Tabor, and the industrial contact was held to give updates on progress and raise any questions. Another meeting was held every week between group members to plan the agenda for the formal meeting and discuss issues and problems faced as well as regular contact between members occurring via email and online messaging.

Individual projects were managed solely by the individual completing them. For this project, a personal Gantt chart was created which comprised of the internal group deadlines as well as additional aspects that related to experimental work and report writing. A log book was

utilised throughout and to record many aspects of the project. In particular the log book was used to record experimental information and data such as: the flow rates in the different tanks, the sample times and data from the samples and propeller-meter used to calculate concentrations and velocities respectively. Additionally the log book also contained information on the measurement points as well as being used to record any information collected over the project.

Over the project there were factors that impacted the progress. The key being: the redesign of the rectangular tank, delays in obtaining simulation results and the computational time required for the Swirl-Flo® which are detailed in Section 3.7. Furthermore, heavy snows resulted in the closure of the fluids laboratory which caused delays with the experimental studies. These factors were mitigated through using float times that were added in initial planning stages.

6.2. Health and Safety

In Section 3.6, the need for consideration of health and safety risks is prerequisite to carrying out experiments is outlined along with the requirement of risk assessments to display proper risk awareness and mitigation.

Examples of hazards that had to be considered are outlined in Section 3.6. Additionally, the storage of OSP needed consideration with the key requirement being avoidance of open flames as OSP, like all flours ignites easily.

As most of the experiments utilised the same equipment and procedures, one broad risk assessment covering the risks such as flooding, electrical appliances and water and OSP with control measures was comprised. Additional risk assessments such as a specific one required for gluing the pipework were created as the need arose. Within labs, it was standard practice to know the locations of the mops, buckets and water vacuums so that in the event of flooding they could be quickly found and utilised.

6.3. Sustainability Considerations

The key environmental and sustainability issue for consideration was the water usage. As outlined in Section 3.6, the experiments carried out required a large amount of water that could not be recirculated. This created several issues to be considered, the key ones being the finite supply of water and the removal of the water after use.

Although the experimental side of this project required a lot of water, the future potential from this completed project is that the company may be able to use simulations more confidently when developing new products and hence reduce the use of clean water. So,

while the water use in this project may not have been sustainable, in the long-term this project could have far-reaching positive effects on water sustainability from the work completed.

7. Contribution to group functioning

As outlined in Section 1.2, the project detailed in this report formed one of seven work packages (or projects) all of which were key to the completion of the group project deliverables. This section details the contributions within the group, namely the contributions of the rest of the group towards this project and the contributions of the author to the other projects and group objectives.

7.1. Group Contribution to Individual Objectives

The group were split into two key sub-teams: experimental and simulation. The experimental sub-team contributed to this project's objectives through collaboration in the experiments outlined in Section 3.3. Primarily with aid from Wye [20] and Mendoza [25] in collecting samples, taking and recording measurements and ensuring both tanks were running correctly. Furthermore, additional work was carried out for the setting up of the experiments, with a whole sub-team contribution for the plumbing in of the Swirl-Flo® inflow and outflows of both tanks. Of note one particular contribution by Wye [20] was the design of the various stands and jigs used and the new hopper and base for the rectangular tank.

The simulation sub-team contributed to this project's objectives through generating results from the simulations which were required for validation. To achieve these results, work was required from all 4 simulation sub-team members with meshes generated by Scobell [26] and Lowe [27] and simulation results achieved by Bentley [19] and Russell [18].

7.2. Contribution to Global Group Objectives

The work completed within this project was crucial for achieving the comparison and validation objective for the group work. The data collected from experiments was used to carry out the comparisons between the two tanks as well as between the simulation and experimental results. Additionally, the work carried on data analysis of concentrations and velocities provided needed information and plots for both the simulation and experimental sub-teams. Further contributions of the author to the group functioning were: health and safety officer (carrying the responsibility of identifying all risks and creating relevant risk assessments) and experimental lab manager (which entailed coordinating the experiments of both tanks and making decisions regarding methods and measurement and sample timings).

References

[1] [Online]. Available: https://dictionary.cambridge.org/dictionary/english/sewage. [Accessed 06 05 2018].

[2] "Sciencing," [Online]. Available: https://sciencing.com/separation-water-sewage-treatment-plants-8397836.html. [Accessed 07 05 2018].

[3] "Wildon," 28 08 2014. [Online]. Available: http://www.wildonuk.co.uk/news/sewage-treatment-process/. [Accessed 07 05 2018].

[4] "SPS Engineering," SPS Engineering, [Online]. Available: http://spsengineering.com/primary-secondary-clarifiers/. [Accessed 08 05 2018].

[5] Partech, [Online]. Available: https://www.partech.co.uk/application/primary-settlement-tanks/. [Accessed 08 05 2018].

[6] "The Constructor Civil Engineering Home," The Constructor, [Online]. Available: https://theconstructor.org/environmental-engg/types-of-sedimentation-tank/14711/. [Accessed 08 05 2018].

[7] M. &. Eddy, Wastewater Engineering Treatment and Resource Recovery Volume 1, McGraw-Hill Education, 2013.

[8] "Dyson," Dyson, [Online]. Available: https://www.dyson.co.uk/vacuum-cleaners.html. [Accessed 08 05 2018].

[9] Hydro International, [Online]. Available: https://www.hydro-int.com/en/products/first-defense?gclid=CjwKCAjwlcXXBRBhEiwApfHGTfjyLt3qA-6DzArLF9QJVkRtC0hjq_l39L0Xg_ZbmlNcecrhAK10tRoCO_MQAvD_BwE. [Accessed 08 05 2018].

[10] L. Svarovsky, "Fluid Flow and Particle Motion in a Hydrocyclone," in *Hydrocyclones*, Holt, Rinehart and Winston, 1984, p. 30.

[11] "Aqualytic," [Online]. Available: http://en.aqualytic.de/products/turbidity-meters. [Accessed 08 05 2018].

[12] "Dantec Dynamics," [Online]. Available: https://www.dantecdynamics.com/measurement-principles-of-lda. [Accessed 23 11 2017].

[13] K. e. al, "High Speed Schlieren by Using Light Emitting Diodes," 2018.

[14] C. G. C. e. al, Modern Developments in Flow Measurement, Peter Peregrinus Ltd, 1971.

[15] codecogs, [Online]. Available: http://www.codecogs.com/library/engineering/fluid_mechanics/pipes/venturi-meters.php. [Accessed 08 05 2018].

[16] A. J. H. e. al., "Cyclone optimisation based on CFD predictions," in *Vortex Separation 5th International Conference on Cyclone Technologies*, BHR Group Limited, 2000, pp. 43-52.

[17] C. A. M. e. al., "Mathematical modelling and experimental validation of flow in a cyclone," in *Vortex Separation 5th International Conference on Cyclone Technologies*, BHR group Limited, 2000, pp. 175-186.

[18] R. T, "The Use of the Drift Flux Model to Simulate a Hydrodynamic Vortex Separator in OpenFOAM," 2018.

[19] B. R, "An Investigation into MULES and its Application into Simulating Settling Behaviour in an Armfield Settling Tank," 2018.

[20] A. Wye, "Investigation and Development of a Mathematical Model to Describe the Settling Characteristics of Olive Stone Powder," 2018.

[21] "Nixon Flow Meters," [Online]. Available: http://www.nixonflowmeters.co.uk/Portals/25/PDF/streamflo.pdf. [Accessed 09 05 2018].

[22] "Vectrino Profiler," Nortek, [Online]. Available: http://www.nortek.no/lib/data-sheets/datasheet-vectrino-profiler. [Accessed 09 05 2018].

[23] Hexagon Geospatial, [Online]. Available: https://www.hexagongeospatial.com/products/power-portfolio/erdas-imagine. [Accessed 12 05 2018].

[24] W. A. R. T. B. R. M. M. L. J. S. T. Baker A, "Experimental and Numerical Investigation into the Use of Olive STone Powder as a substitute for Primary Sludge Modelling," 2018.

[25] M. M, "Determination of a Viscosity Model for an Olive Stone Powder and Water Suspension for Primary Sedimentation Tank Modelling," 2018.

[26] S. T, "Investigation into Mesh Generation Techniques Using Pointwise on Primary Sewage Sedimentation Devices," 2018.

[27] L. J, "Investigation into mesh generation using snappyHexMesh for a model Sedimentation Tank and Hydrodynamic Vortex Flow Separator including Volume of Fluid Simulation," 2018.